An Electron Density Model above the Sunspot from a Mapping of NOAA 7260 at 17 GHz

Xing-Feng Yu[1,2] $\star$ and Jin-Xing Yao[1]

[1] Purple Mountain Observatory, Chinese Academy of Sciences, Nanjing 210008
[2] National Astronomical Observatories, Chinese Academy of Sciences, Beijing 100012

Abstract   The brightness temperature distribution of microwave emission in a solar active region generally shows a ring structure, with a dip at the centre. However, no dip was found in the Nobeyama Radioheliograph left handed circular polarization (LCP) image on 1992 August 18; instead, there was a peak. This is a completely LCP source with zero right-handed circular polarization (RCP). We examine this structure in terms of the joint effect of gyroresonance and bremsstrahlung mechanism with a raised electron density above the central part of the sunspot, and the commonly assumed temperature and vertical dipole magnetic field models. The raised electron density is found to be $1.4 \times 10^{11}\,\mathrm{cm}^{-3}$ at the chromosphere base.

Key words: Sun: activity — sunspots — Sun: radio radiation — Sun: chromosphere

1   INTRODUCTION

The emission of the solar radio slowly varying component (SVC) has been studied extensively by a number of authors, and a succession of theories have been constructed (Zheleznyakov 1970; Zlotnik 1968a, b; White & Kundu 1997). The SVC emission owes its origin to radio sources in active regions on the solar disk. It is known that at shorter wavelengths ($\lambda < 10\,\mathrm{cm}$) the sources are closely related to the sunspots. The SVC emission at short centimeter wavelengths from the sources in the chromosphere and corona above the active regions is generally dominated by gyroresonance opacity. Images computed according to the theory of gyroresonance emission and assuming a solar atmosphere model, show peculiar structures like a ring or horseshoe, that are consistent with the observations at centimeter wavelengths (Zlotnik 1968b; Zhao & Qian 1982). However, some recent high-resolution observations have shown that some images at 14.7 GHz can be explained by bremsstrahlung emission (Zlotnik et al. 1998). In this paper, using high-resolution Nobeyama Radioheliograph data at 17 GHz, we argue that at short centimeter wavelengths the SVC emission is caused by the combined mechanism of both

---

$\star$ E-mail: pmoyxf@263.net

bremsstrahlung and gyroresonance radiations, and we further infer that the electron density is significantly greater in the central part of the sunspot than at its edge.

2   OBSERVATIONAL DATA

The radio source was located above the active region NOAA 7260 which just passed the central meridian on 1992 August 18. Figure 1 shows partial images of the active region in LCP (a) and RCP (b) at 0325 UT on 1992 August 18 by the Nobeyama Radioheliograph quoted from Shibasaki et al. (1994). It can be seen from Figure 1 that the compact radio source (source A) has only an LCP component (a), and its RCP component (b) is zero, so its degree of polarization is nearly 100%. Figure 2 shows the plot of brightness temperature T_b versus position for the section along the line shown in Figure 1 (a). Figure 2 shows that the brightest part in source A is at the centre and no dip can be found within it. This is different from sources observed at lower frequencies where we find the so-called ring or horseshoe structures.
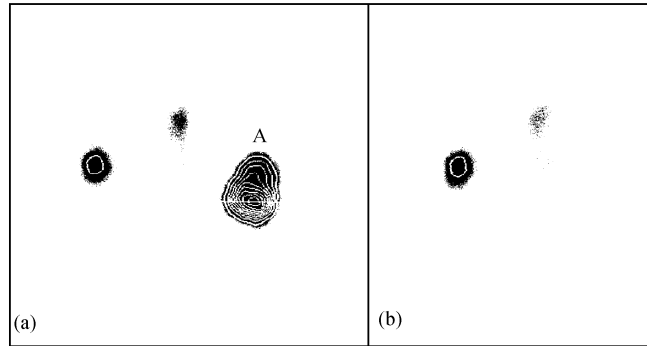

Fig. 1   Partial images of the active region NOAA 7260 at 0320 UT on 1992 August 18 observed at 17 GHz by the Nobeyama Radioheliograph (after Shibasaki 1994). (a) Radio brightness temperature distribution in LCP in both gray scale and contours. (b) Same as (a) but for RCP.

3   A MODEL OF THE ACTIVE REGION

Gyroresonance emission arises in very thin layers of constant magnetic field strength, B, corresponding to the resonance $f = sf_B = 2.8 \cdot s \cdot B$ (MHz), s being the integer harmonic number. For $f = 17$ GHz and $s = 1, 2, 3, 4$, B is 6071 G, 3036 G, 2024 G and 1518 G, respectively. There are no magnetic fields in the chromosphere and corona as high as the values for $s = 1$ and 2. For $s \geq 4$, the optical thickness is approximately zero (see text below). Accordingly we only need to consider the contribution from the $s = 3$ harmonic layer to the 17 GHz emission.

The adopted magnetic field in this paper is approximately represented by a vertical dipole submerged to a depth d in the photosphere. Figure 3 shows the $s = 3$ gyroresonance layer for different d. We see that for $d \leq 3.5 \times 10^9$ cm the resonance layer radius from the center to the point where the resonance layer intersects the choromosphere base, (2000 km above the photosphere), is less than the radius in the observed image. The observed radius is 1.68×10^9 cm

for the section in Figure 1 (see Figures 2 and 3). For $d > 4 \times 10^9$ cm both the height and radius of the resonance layer at the center are larger. Therefore we only calculate the brightness distribution for $d = 4 \times 10^9$ cm.

The models of temperature T and electron density N are shown in Figure 4 (Zlotnik et al. 1996, 1998). The temperature model has exponential dependence on the height, while the electron density model has exponential dependence on both the height and radius.
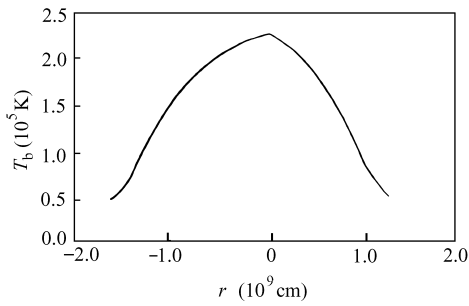

Fig. 2   Plot of brightness temperature T_b versus position for the section along the line in Figure 1 (a).
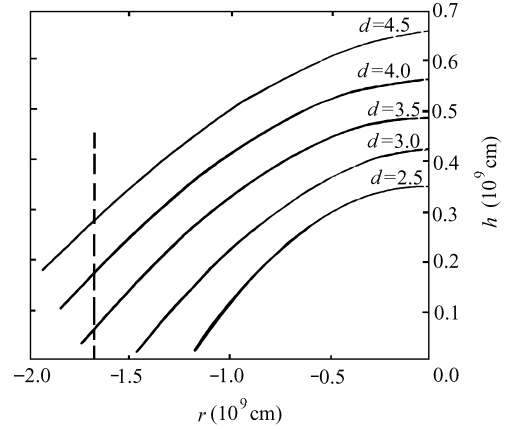

Fig. 3   Curves of the third harmonic gyroresonance layer for the emission at 17 GHz for the different values of dipole moment d (in unit of 10^9 cm) labelled alongside. Horizontal axis is distance r measured from the spot center. Vertical axis is height above the photosphere and the vertical dashed line marks the left radius in Figure 2.

4   EMISSION MECHANISM

4.1   Gyroresonance Emission

As mentioned above we only consider the emissions from the third harmonic layer. For $s = 3$, the optical thickness for gyroresonance opacity is given by Zlotnik (1968a)

$$\tau_{j3} = 0.3829 \times 10^{-6} N T^2 \lambda L_H \frac{\sin^4 \theta (\sin^2 \theta + 6 \cos^2 \theta \pm \sqrt{\sin^4 \theta + 36 \cos^2 \theta})^2}{\sin^4 \theta + 36 \cos^2 \theta \pm \sin^2 \theta \sqrt{\sin^4 \theta + 36 \cos^2 \theta}} , \qquad (1)$$

where for the extraordinary wave, we take $j = I$ and the upper sign and for ordinary wave, $j = II$ and the lower sign, λ is the wavelength expressed in cm, L_H the characteristic scale of the magnetic field, and θ the angle between the magnetic field and the line of sight.

The brightness temperature of the gyroresonance emission for $s = 3$ is given by Zlotnik (1968a)

$$T_{bI} = T_3 (1 - e^{-\tau_{I3}}) e^{-\tau_{14}} + T_4 (1 - e^{-\tau_{14}}) , \qquad (2)$$

$$T_{bII} = T_3 (1 - e^{-\tau_{II3}}) . \qquad (3)$$

4.2   Bremsstrahlung Radio Emission

Because the bremsstrahlung emission of electrons occurs through the entire thickness of the chromosphere and corona, we need to consider the inhomogeneity of the solar atmosphere. The optical thickness σ_j, the brightness temperature θ_j and the absorption coefficient μ_j of bremsstrahlung-generated radio emission are, respectively (Zlotnik 1968a),

$$\sigma_j = \int \mu_j \mathrm{d}h\,, \tag{4}$$

$$\theta_j = \int T \mathrm{e}^{-\sigma_j} \mathrm{d}\sigma_j\,, \tag{5}$$

$$\mu_j \approx \frac{1.041 Q \lambda^2 N^2}{T^{3/2}} f(\theta)\,. \tag{6}$$

Here

$$Q = \ln \frac{220T}{N^{1/3}}\,, \qquad T < 3 \times 10^5 \mathrm{K}\,,$$

$$Q = \ln \frac{10^3 T^{2/3}}{N^{1/3}}\,, \qquad T > 3 \times 10^5 \mathrm{K}\,,$$

$$f(\theta) = \frac{E[2(1-v)^2 + u \sin^2 \theta] - u^2 \sin^4 \theta}{E[2(1-v)^2 - u \sin^2 \theta + E]^{1/2}}\,,$$

$$E = \mp \sqrt{u^2 \sin^4 \theta + 4u(1-v)^2 \cos^2 \theta}\,,$$

$$u = \frac{\omega_B^2}{\omega^2}\,, \quad v = \frac{\omega_{pe}^2}{\omega^2}\,, \quad \omega = 2\pi f\,, \quad \omega_B = 2\pi f_B \quad \text{and} \quad \omega_{pe} = 2\pi f_{pe}\,.$$

We write f_{pe} for the plasma frequency, and assume the refractive index $n_j \sim 1$. The total brightness temperature of the radio emission by the joint effect of the bremsstrahlung and gyroresonance mechanisms is given by Zlotnik (1968b)

$$T_{bI} = [\theta_{Ip3} \mathrm{e}^{-\tau_{I3}} + \theta_{I34}] \mathrm{e}^{-\tau_{I4}} + \theta_{I4} + T(h_3)(1 - \mathrm{e}^{-\tau_{I3}}) \mathrm{e}^{-\sigma_{I3} - \tau_{I4}} + T(h_4)(1 - \mathrm{e}^{-\tau_{I4}}) \mathrm{e}^{-\sigma_{I4}}, \tag{7}$$

$$T_{bII} = \theta_{IIp3} \mathrm{e}^{-\tau_{II3}} + \theta_{II3\infty} + T(h_3)(1 - \mathrm{e}^{-\tau_{II3}}) \mathrm{e}^{-\sigma_{II3}}\,, \tag{8}$$

where σ_{j3} (σ_{j4}) represents the optical thickness of the solar atmosphere from the $s = 3$ ($s = 4$) level to emergence from the corona, and θ_{jp3} the brightness temperature of bremsstrahlung radio emission generated on the layer between the levels of the photosphere and $s = 3$ harmonic for wave j, θ_{j34} is that in the region between the 3rd and 4th harmonics.

5   RESULTS AND DISCUSSION

The one-dimensional radio brightness temperature distribution of the radio source along the radius r from the central part of the sunspot computed with Eqs. (1)–(7) for X-mode is shown in Figure 5. Curve b in Figure 5 was obtained using the electron density model $N(h, r)$ in Figure 4 and the joint mechanism of the gyroresonance and bremsstrahlung emissions according to Eq.(7). Curve c was obtained using only the electron density $N(h) = N(h, 0.64)$ in Figure 4 and the gyroresonance Eq. (2). It can be seen from Figure 5 that curve (b) basically coincides with the observed curve (a), while curve (c) coincides with curve (a) only for $r < -1.25 \times 10^9$ cm: In this part, curves (b) and (c) coincide. In fact, for $r < -1.25 \times 10^9$ cm, the

contribution of bremsstrahlung emission is negligible, while gyroresonance emission makes the main contribution. However, for $r > -1.25 \times 10^9$ cm, the bremsstrahlung emission still plays a partial role because of the increased electron density. This shows that the central peak of the radio image at 17 GHz is caused by the joint effect of the two mechanisms.
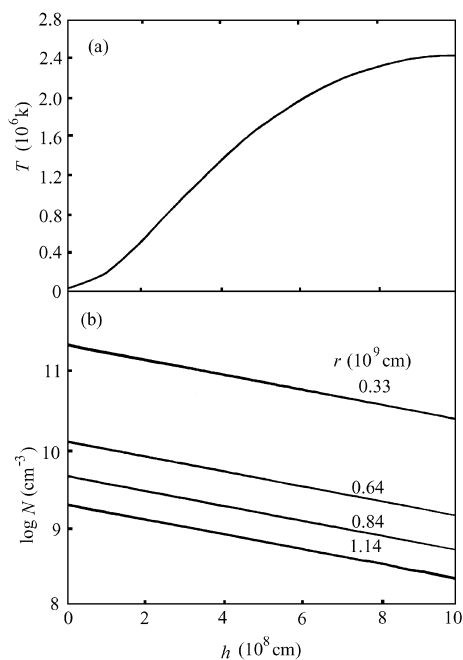

Fig. 4   Adopted models in the solar atmosphere. (a) Temperature model only depends on height; (b) Density model depends on both height (h) and radius (r).
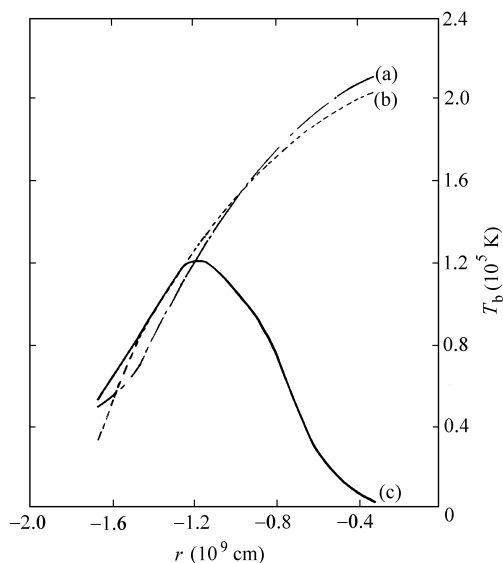
Fig. 5   Radio brightness temperature distribution versus radius at 17 GHz. (a) Observed; (b) Computed with the $N(h, r)$ of Figure 4 and the joint mechanism of gyroresonance and bremsstrahlung emissions. (c) Computed with $N(h, 0.64)$ and the gyroresonance emission.

According to the theory of gyroresonance emission, the brightness temperature "dip" in the central part of the radio image is caused by a small angle θ at the center ($\theta < 10°$), that is, a very thin optical thickness. In order to explain the observed peak brightness temperature at the center, we must increase the temperature or the electron density to increase the optical thickness. The soft X-ray emission observed on 1992 August 18 was very weak (Shibasaki 1994), and the temperature required by the model is higher (about $5 - 7 \times 10^6$ K), hence we adjust the electron density N to increase the optical thickness. The electron density N by our calculation is 1.4×10^{11} cm^{-3}; this result is consistent with that of Zlotnik et al. (1998).

The calculation shows that the gyroresonance emission for O-mode is approximately zero. The bremsstrahlung emission for O-mode is about 3–5 times less than that of X-mode, so the joint mechanism of both emissions for O-mode is almost zero. This confirms the observed pure polarization.

We note that the proposed model in this paper is still far from complete because the available

image for our analyse is only from a single frequency. The principal result is that above the sunspot center there is a dense plasma whose temperature is the same as that of the adjacent plasma.

References

Alissandrakis C. E., Kundu M. R., 1982, ApJ, 253, L49

Shibasaki S., Enome S., Nakajima H. et al., 1994, PASJ, 46, L17

White S. M., Kundu M. R., 1997, Solar Phys., 174, 31

Zhao R. Y., Qian S. J., 1982, Acta Astronomica Sinica, 23, 34

Zheleznyakov V. V., 1970, Radio Emission of the Sun and Planet, Pergamon Press

Zlotnik E. Ya., 1968a, Soviet Astronomy, 12, 245

Zlotnik E. Ya., 1968b, Soviet Astronomy, 12, 463

Zlotnik E. Ya., Kundu M. R., White S. M., 1996, Radiophysics and Quantum Electronics, 39, 255

Zlotnik E. Ya., White S. M., Kundu M. R., 1998, ASP Conference Series, 155, 135